



# Host translesion polymerases are required for viral genome integrity

Sebastian Zeltzer<sup>a</sup>, Pierce Longmire<sup>b,c</sup>, Marek Svoboda<sup>d</sup>, Giovanni Bosco<sup>d</sup>, and Felicia Goodrum<sup>a,b,c,1</sup>

Edited by Thomas Shenk, Princeton University, Princeton, NJ; received February 23, 2022; accepted June 8, 2022

Human cells encode up to 15 DNA polymerases with specialized functions in chromosomal DNA synthesis and damage repair. In contrast, complex DNA viruses, such as those of the herpesviridae family, encode a single B-family DNA polymerase. This disparity raises the possibility that DNA viruses may rely on host polymerases for synthesis through complex DNA geometries. We tested the importance of error-prone Y-family polymerases involved in translesion synthesis (TLS) to human cytomegalovirus (HCMV) infection. We find most Y-family polymerases involved in the nucleotide insertion and bypass of lesions restrict HCMV genome synthesis and replication. In contrast, other TLS polymerases, such as the polymerase  $\zeta$  complex, which extends past lesions, was required for optimal genome synthesis and replication. Depletion of either the pol $\zeta$  complex or the suite of insertion polymerases demonstrate that TLS polymerases suppress the frequency of viral genome rearrangements, particularly at GC-rich sites and repeat sequences. Moreover, while distinct from HCMV, replication of the related herpes simplex virus type 1 is impacted by host TLS polymerases, suggesting a broader requirement for host polymerases for DNA virus replication. These findings reveal an unexpected role for host DNA polymerases in ensuring viral genome stability.

herpesvirus | TLS polymerase | genome replication | cytomegalovirus | DNA repair

Bacteria, fungi, and animals encode a plethora of DNA-dependent DNA polymerases (1). The diversity of polymerases in a single organism mirrors the varied configurations and geometries of DNA molecules. Processive polymerases of the B-family are high-fidelity enzymes that perform most chromosomal synthesis; their accuracy comes from the synergy of a narrow binding pocket, mediating correct nucleotide insertion, and 3'-5' exonuclease activity for error processing (2, 3). Alternately, Y-family translesion DNA synthesis (TLS) polymerases (pols) with enlarged binding pockets and no proofreading function have reduced enzymatic idling and can synthesize through warped DNA landscapes containing adducts, cross-links, dimers, or abasic sites (4–7).

Of the 15 DNA polymerases encoded by humans, 5 have been identified as performing TLS. The Y-family TLS polymerases include pol $\eta$ , pol $\kappa$ , pol $\iota$ , and Rev1 (8). The fifth TLS pol, pol $\zeta$  (composed of Rev3L and Rev7) is a B-family polymerase that, unlike pol $\epsilon$  or pol $\delta$ , lacks 3'-5' exonuclease proofreading (9). Genetic studies indicate that while TLS polymerases are essential for resistance to DNA damaging agents, their lack of proofreading and larger active sites result in mutation (1, 10).

Some double-stranded DNA (dsDNA) viruses, including *herpesviridae*, encode a single B-family DNA-dependent DNA polymerase (11, 12). These polymerases have 3'-to-5' exonuclease activity, which ensures replication fidelity and integrity (13, 14). However, these viral polymerases replicate DNA with limited ability to repair damage to their genomes that occurs during replication. A role for host DNA polymerases in the replication of viruses that encode their own polymerase has been little explored. Human cytomegalovirus (HCMV) is a  $\beta$ -herpesvirus, with a slow life cycle and a large dsDNA genome of ~236 kb. Like all herpesviruses, HCMV establishes a life-long latent infection in the host, increasing the likelihood that viral genomes may accumulate damage. Additionally, HCMV genomes have complex geometries rich with repeated sequences and a high proportion of guanine–cytosine nucleotide bonds (57% GC) that have the potential to support G-quadruplex formation implicated in the regulation of viral gene expression (15). HCMV DNA synthesis occurs in specialized nuclear compartments termed viral replication centers (RC). RCs are biomolecular condensates largely segregated from host DNA that grow in both size and complexity as genomes are amplified (16–18). While spatially distinct and regulated by numerous viral proteins, viral DNA is subject to the same insults that induce host DNA lesions. Consistent with this, numerous studies have indicated HCMV coopts DNA damage repair and tolerance proteins, often recruiting them to RCs (19–21).

## Significance

Double-stranded DNA (dsDNA) viruses, such as herpesviruses, encode DNA-dependent polymerases of the B family, which due to their structure, are insufficient for synthesizing through DNA with lesions. Anticipating that DNA lesions present a problem to dsDNA viruses, we wondered if viral polymerases were truly sufficient for viral genome replication. We tested the importance of a specialized class of translesion polymerases (TLS) for human cytomegalovirus (HCMV) replication, and that of other dsDNA viruses. TLS polymerases have distinct roles in viral replication and are important for HCMV genome stability. Our results provide a new perspective on DNA virus life cycles and implicate TLS polymerases as a viral target, underscoring yet another viral assault to host biology.

Author affiliations: <sup>a</sup>BIOS Institute, University of Arizona, Tucson, AZ 85721; <sup>b</sup>Graduate Program in Molecular Medicine, University of Arizona, Tucson, AZ 85721; <sup>c</sup>Department of Immunobiology, University of Arizona, Tucson, AZ 85721; and <sup>d</sup>Department of Molecular and Systems Biology, Dartmouth Geisel School of Medicine, Hanover, NH 03755

Author contributions: S.Z., P.L., M.S., G.B., and F.G. designed research; G.B. and F.G. directed the research; S.Z., P.L., M.S., and G.B. performed research; S.Z., P.L., and M.S. contributed new reagents/analytic tools; S.Z., P.L., M.S., G.B., and F.G. analyzed data; and S.Z., P.L., G.B., and F.G. wrote the paper.

The authors declare no competing interest.

This article is a PNAS Direct Submission.

Copyright © 2022 the Author(s). Published by PNAS. This article is distributed under Creative Commons Attribution-NonCommercial-NoDerivatives License 4.0 (CC BY-NC-ND).

<sup>1</sup>To whom correspondence may be addressed. Email: fgoodrum@arizona.edu.

This article contains supporting information online at <http://www.pnas.org/lookup/suppl/doi:10.1073/pnas.2203203119/-DCSupplemental>.

Published August 10, 2022.

Using HCMV as a model system, we sought to understand how DNA viruses replicate their genomes with a single polymerase when their host requires 15. We found that HCMV altered the subcellular distribution of TLS polymerases. In support of their activation, infection induced the monoubiquitylation of proliferating cell nuclear antigen (PCNA). While PCNA serves as a processivity factor for bulk DNA synthesis, its monoubiquitylated form is important for the recruitment of TLS polymerases to sites of damage (22–24). We found that TLS polymerases functioned in HCMV replication and genome synthesis, and specific TLS polymerase roles varied between restricting and facilitating viral replication. In aggregate, *polη*, *polκ*, and *polι* restricted HCMV replication, while Rev1, Rev3L, and Rev7 were required for optimal HCMV replication. However, all TLS polymerases played a role in minimizing viral genomic rearrangements occurring at regions with high GC content and regions rich in repeated sequences. We extended our investigation to other dsDNA viruses and found that the  $\alpha$ -herpesvirus, herpes simplex type 1 (HSV1), required *polη*, *polκ*, and *polι* for optimal replication, suggesting divergent processes for viral replication. This work investigates a fundamental assumption in how dsDNA viruses replicate their genetic material and introduces a class of proteins parasitized by DNA viruses, TLS polymerases.

## Results

**HCMV Recruits Host Translesion Polymerases and Monoubiquitinates PCNA in HCMV Infection.** HCMV has been described as parasitizing numerous host DNA repair/tolerance proteins, possibly to overcome a deficit of virally encoded homologs; importantly, many of these proteins have been observed concentrated at RCs (19, 20, 25). We asked if HCMV might recruit Y-family TLS polymerases to RCs to compensate for constraints imposed by the structure of its own B-family polymerase, UL54, in resolving DNA damage or synthesizing through DNA with complex geometries. We examined the localization of Y-family polymerases in HCMV-infected primary fibroblasts relative to the viral DNA processivity homolog, pUL44, which marks RCs. HCMV infection altered the distribution all four Y-family polymerases (Fig. 1A). In uninfected cells, *polη* was distributed throughout the nucleus, while *polι* was largely at the margins of RC-infected cells. *Polι* was concentrated as one to two foci per cell in both uninfected and HCMV-infected cells, but the puncta were generally proximal to RCs in infected cells. *Polκ* formed irregular foci in the nuclei of uninfected cells but appeared restricted to the periphery of RCs in HCMV-infected cells. Rev1 was distributed throughout the nucleus but showed considerable coassociation with RCs in HCMV infection. Of note, viral DNA synthesis occurs at the margins of RCs, indicating that polymerases observed near these locations are proximal to regions of active synthesis (26). These results indicate that infection with HCMV broadly reorganizes the location of Y-family TLS polymerases, concentrating them at or near sites of viral DNA synthesis.

Y-family polymerases are recruited to DNA lesions via the monoubiquitination of PCNA (27–29). Therefore, we analyzed the ratios of total and monoubiquitinated PCNA in uninfected and HCMV-infected fibroblasts over a 96-h time course. PCNA concentration negatively correlated with confluency in uninfected cells, a phenomenon consistent with increased contact inhibition (Fig. 1B, quantified in Fig. 1C) (28). In contrast, PCNA levels were stable over the 96-h time course of HCMV infection. Furthermore, using a monoubiquitin-specific PCNA antibody over a time course of infection, we found that Ub-PCNA accumulated

over the course of infection at times consistent with viral DNA synthesis (Fig. 1D, quantified in Fig. 1E). Consistent with this, Ub-PCNA was increasingly enriched in nuclear chromatin-bound fractions over the course of infection (Fig. 1F, quantified in Fig. 1G), but not in uninfected cells. PCNA also accumulated within nuclear viral RCs that are marked by the viral DNA processivity factor, pUL44 (Fig. 1H). While both PCNA and pUL44 localize to RCs, they do not precisely colocalize, suggesting they may be in distinct domains performing separate functions. Taken together, these results indicate that HCMV creates conditions consistent with the activation of the TLS pathway, culminating in the reorganization of Y family polymerases and their regulator, PCNA.

**Depletion of Y Family TLS Polymerases Differentially Impacts Viral Replication.** We next sought to define the significance of Y-family TLS polymerases to the HCMV lifecycle. We generated lentiviral short-hairpin RNA (shRNA) pools against each polymerase to stably knockdown *polη*, *polκ*, *polι*, or Rev1 in growth-arrested fibroblasts. Importantly, infected fibroblasts do not synthesize host DNA and, therefore, knockdown of these polymerases should not impose stress on host cells. A construct expressing an shRNA specific to luciferase (Luc) was used as a nonspecific control. We achieved ~50% knockdown for each polymerase (Fig. 2A). Cells were infected and viral genome accumulation and replication was measured. While depletion of *polκ*, *polι*, or *polη* trended toward enhancing viral genome synthesis and production of infectious virus (each individual replicate yielded higher genomes/titers than controls), a high degree of experimental variation culminated in nonsignificant results for each knockdown (Fig. 2B and C). Strikingly, the loss of Rev1 resulted in significantly diminished viral genomes and titers (Fig. 2B and C).

TLS polymerases compete for binding at lesions (30). Based on this we wondered if knockdown of a single insertion polymerase resulted in an incomplete phenotype due to rescue via the remaining insertion polymerases. To test this, we knocked down *polη*, *polκ*, and *polι* in aggregate. We found that combined loss of *polη*, *polκ*, and *polι* resulted in significant increases in viral yields relative to the Luc knockdown control (Fig. 2D). As their combined loss would be more likely to ensure ablation of any possible overlapping function, we opted to use pooled knockdowns of *polη*, *polκ*, and *polι*, denoted as *pol(η,κ,ι)*, for future experiments. Taken together, these results suggest Y-family polymerases *polη*, *polκ*, and *polι* restrict viral genome synthesis and the production of infectious progeny in a manner that may be compensatory. In stark contrast to its family members, Rev1 was important for efficient viral genome synthesis and replication.

**Rev1 and Polζ Facilitate HCMV Replication.** Rev1 is divergent from other Y-family polymerases in that its catalytic activity is dispensable for its role in TLS (28). Distinct from its polymerase activity, Rev1 also acts as a scaffolding protein that facilitates a polymerase switching event. *Polη*, *polκ*, and *polι* are exchanged following nucleotide insertion opposite a lesion for the B-family polymerase, *polζ* (consisting of the catalytic subunit Rev3L and its adaptor Rev7). Rev1 acts as a scaffold allowing *polζ* to extend past or bypass a lesion (9, 31). We hypothesized that the viral replication defects observed with loss of Rev1 were related to its role in regulating *polζ* activity. To test this, we generated shRNA against Rev3L and Rev7 to knockdown *polζ* and verified >50% knockdown relative to Luc (Fig. 3A) (6). We found that loss of Rev3L or Rev7 phenocopied loss of Rev1, resulting in significantly diminished viral genomes and yields (Fig. 3B and C).

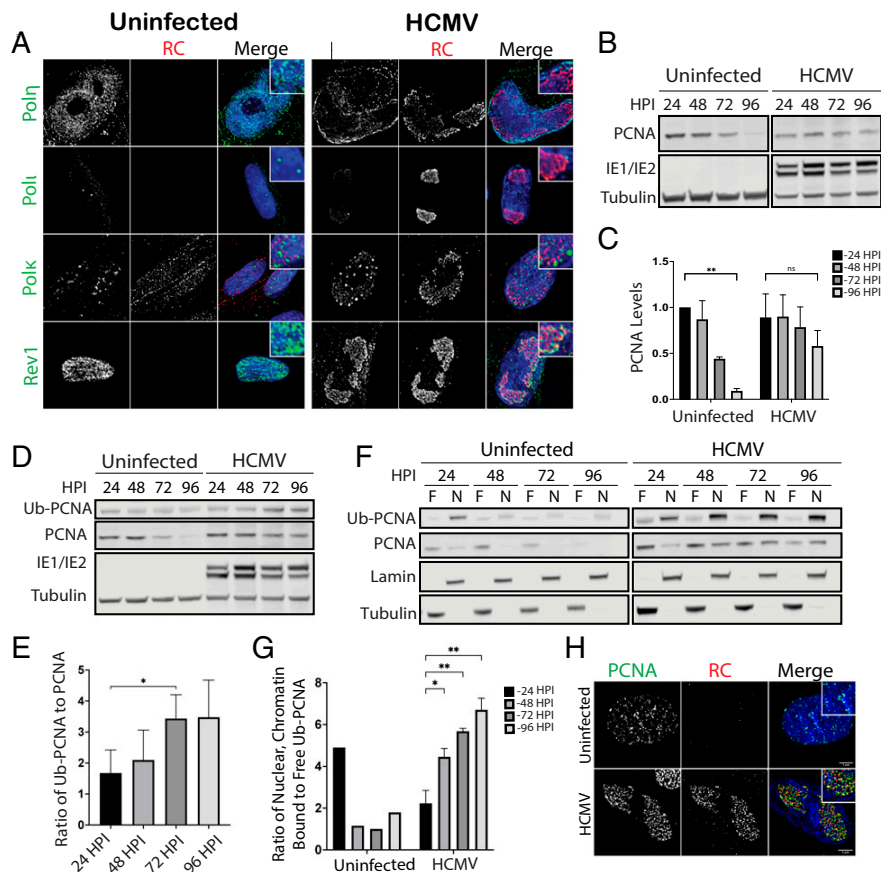


**Fig. 1.** Infection with HCMV results in TLS pol recruitment to RCs. Fibroblasts were mock-infected or infected with HCMV TB40/E at a multiplicity of infection (MOI) of 1. (A) At 72 h postinfection (HPI), cells were fixed and processed for immunofluorescence. All polymerases (green) indicated were indirectly detected with monoclonal antibodies specific to each. RCs (red) were labeled using antibody to pUL44 in the case of pol $\eta$ , pol $\iota$ , or Rev1 or FANCD2 in the case of pol $\kappa$ , and secondary antibodies were conjugated to Alexa Fluor 546 (green) or 647 (red). Coverslips were imaged using a DeltaVision deconvolution microscope. All images correspond to a single focal plane. A merged image with a higher-magnification inset of each channel plus DAPI staining to indicate nuclei is shown on the right of single-color panels. Magnification: 600 $\times$ . (B–G) Uninfected or HCMV-infected cell lysates were collected at 24, 48, 72, and 96 HPI to analyze PCNA by immunoblotting using monoclonal antibodies. Immediate-early proteins (IE1 and IE2) are shown as a control for infection and tubulin is used as a loading control. (B) Total PCNA was analyzed over time in uninfected or HCMV-infected cells. (C) PCNA band intensity was quantified and normalized to tubulin and then to that of uninfected cells at 24 HPI. (D) Ub-PCNA was analyzed over time. (E) The ratio of Ub-PCNA to PCNA band intensity was quantified and normalized to tubulin at each time point. (F) Lysates were prepared from free, soluble (F lanes) and nuclear, chromatin-bound (N lanes) fractions isolated over a time course of infection. Tubulin and lamin serve as fractionation and loading controls. (G) PCNA band intensity was quantified and normalized to tubulin for soluble fractions and lamin for chromatin bound fractions. The y axis depicts a ratio of chromatin bound to soluble Ub-PCNA. Bars on all graphs for quantifications represent the average over three or more independent replicates with SD shown, except for 96 HPI in F represents two replicates. Statistical significance was determined by two-way ANOVA with Tukey's multiple comparisons test in C and G. In E, statistical significance was determined with two-tailed, paired t test with Bonferroni's correction. Asterisks (\*\* $P < 0.001$ , \*\*\* $P < 0.0001$ ) represent statistically significant differences determined in three or more independent experiments. (H) PCNA (green) and pUL44 (red) were localized using monoclonal antibodies to each and secondary antibodies conjugated to Alexa Fluor 546 (green) or 647 (red) and imaged as described for A.

Observing similar phenotypic outcomes when targeting individual subunits indicates that the pol $\zeta$ /Rev1 pathway is important to infection. Consistent with this, the combined loss of all three subunits—Rev3L, Rev1, and Rev7—resulted in a growth defect in synthesis of viral genomes and production of progeny virus (Fig. 3 D and E). To increase the chances of impairing the Rev1/pol $\zeta$  pathway, we opted to employ aggregate knockdown of Rev3L, Rev1, and Rev7 (pol $\zeta$ /Rev1) over targeting a single subunit for future assays.

Considering the requirement of Pol $\zeta$ /Rev1 for optimal virus replication, we next analyzed the distribution of Rev3L catalytic subunit in infection reasoning that it may be recruited to viral RCs similarly to Rev1. In uninfected cells, Rev3L was broadly excluded from the nucleus. Interestingly, Rev3L was concentrated almost exclusively within RCs, forming distinct foci (Fig. 3G). Taken together, these results indicate that the pol $\zeta$ /Rev1 complex

relocalizes proximal to sites of viral DNA synthesis and is important for HCMV genome synthesis and virus replication.

BLAST analysis indicated that the shRNA sequences chosen only had a significant match to the targeted polymerase (E values  $> 1.0$  for nontarget matches). However, to ensure that our shRNA knockdowns resulted in reduced protein target levels but did not have off-target effects, we measured the concentrations of three polymerases for which antibodies are available for immunoblotting (pol $\eta$ , pol $\iota$ , and Rev1) when any one was knocked down individually (SI Appendix, Fig. S1). While target protein levels dropped by 35 to 65% in each knockdown, levels of the other two polymerases measured were relatively unchanged. Attempts to rescue knockdown phenotypes by overexpression of shRNA-resistant clones of TLS polymerases were unsuccessful and resulted in conditions that impaired infection, as indicated by fewer GFP $^{+}$  cells following infection. This may be due to DNA

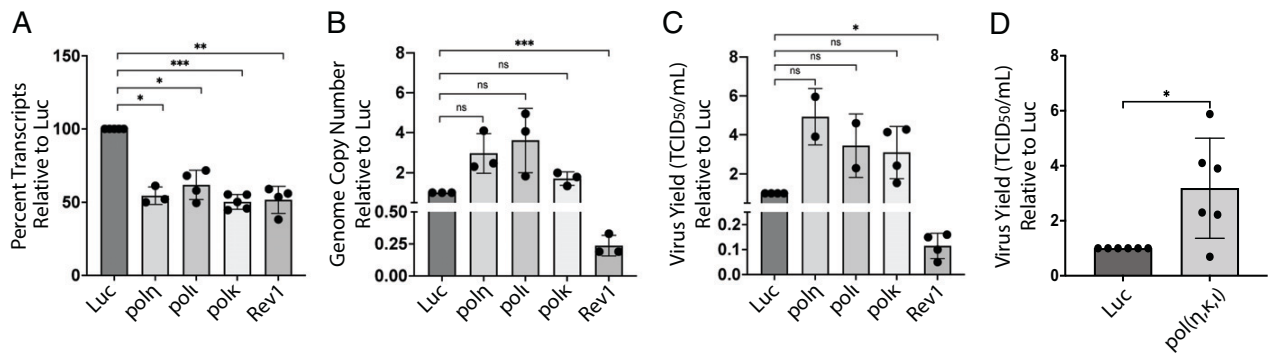


**Fig. 2.** Y-family polymerases differentially influence HCMV replication. (A–C) Growth-arrested primary fibroblasts were transduced with shRNA lentiviruses targeting Luc or respective Y-family polymerase: pol $\eta$ , pol $\iota$ , pol $\kappa$ , or Rev1. Forty-eight hours later, media was refreshed with puromycin at 2  $\mu$ g/mL to select for transduced cells. (A) Twenty-four hours later, cells were infected with HCMV at an MOI of 0.001. Cells were lysed at 16 d postinfection (DPI) and RNA was processed for reverse-transcriptase-qPCR (RT-qPCR). Relative knockdown of transcripts was determined using  $\Delta\Delta$ Ct analysis between luciferase and experimental conditions. The housekeeping transcript, H6PD, was used as a control for cell number. Absolute values are an average of three to five replicates of  $2^{\Delta\Delta$ Ct. (B and C) Following transduction, as described above, knockdown cells were infected with HCMV at an MOI of 0.001 and cells were lysed at 16 DPI. (B) Viral genome copy number for each knockdown was determined by qPCR using a BAC standard curve and a primer to the  $\beta$ 2.7 region of the viral genome relative to the luciferase knockdown control. (C) Viral yields were measured by TCID<sub>50</sub> and normalized to Luc control. (D) Growth-arrested fibroblasts were transduced with shRNA lentiviruses targeting Luc or the combined insertion pol( $\eta,\kappa,\iota$ ) at cumulative MOI of 9. Forty-eight hours later media was refreshed with puromycin at 2  $\mu$ g/mL; 24 h later, cells were infected with HCMV TB40/E at an MOI of 1. Lysates were collected at 4 DPI and viral titers determined by TCID<sub>50</sub>. (A–D) Bars represent the average of three to six independent experiments where dots represent each independent replicate. Statistical significance was determined by two-tailed, paired *t* test with Bonferroni correction; asterisks (\**P* < 0.01, \*\**P* < 0.001, \*\*\**P* < 0.0001) represent statistically significant differences relative to the Luc.

damage or increased mutational burden that may induce intrinsic or innate responses from overexpression of TLS polymerases that would be expected to prevent infection (25, 32).

To confirm that the knockdown of host polymerases indeed resulted in defects in viral genome synthesis and viral replication and were not the result of defects in entry or earlier events in infection, we determined the copy number of intracellular

viral genomes following infection and analyzed the accumulation of the IE1 and IE2 intermediate-early or UL44 early proteins. Knockdown of pol( $\eta,\kappa,\iota$ ) or pol $\zeta$ /Rev1 does not result in a defect in entry as reflected in the number of intracellular viral genomes (*SI Appendix, Fig. S2A*) or a defect in immediate-early (IE1/2) or early gene (UL44) expression (*SI Appendix, Fig. S2B*). While polymerase knockdown did not alter viability of

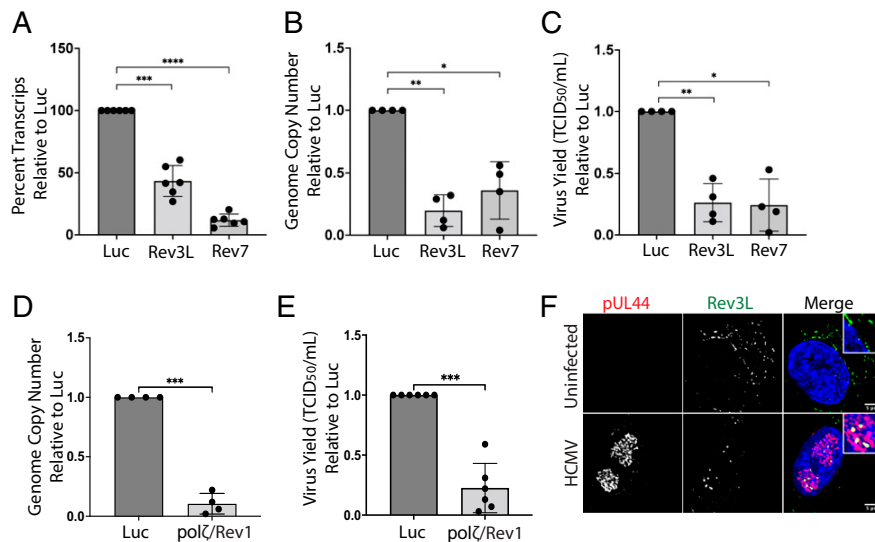


**Fig. 3.** Rev1 and pol $\zeta$  facilitate HCMV replication. (A–C) Growth-arrested primary MRC5 fibroblasts were transduced with shRNA lentiviruses against Luc, or Rev3L or Rev7 at an MOI of 3. Forty-eight hours later, media was refreshed with puromycin at 2  $\mu$ g/mL; 24 h later, cells were infected with HCMV at an MOI of 0.001. (A) RNA was isolated for cDNA synthesis at 20 DPI. Knockdown was quantified by RT-qPCR as described in Fig. 2A. (B and C) Knockdown cells indicated were infected with HCMV at an MOI of 0.001 and cells were lysed at 16 DPI. (B) Viral genome copy number for each knockdown was determined by qPCR using a BAC standard curve and a primer to the  $\beta$ 2.7 region of the viral genome relative to the Luc knockdown control. (C) Viral yields were measured by TCID<sub>50</sub> and normalized to Luc control. (D and E) Growth-arrested fibroblasts were transduced with shRNA lentiviruses targeting Luc or the combined Rev3L + Rev7 (pol $\zeta$ ) and Rev1 at a cumulative MOI of 9. Forty-eight hours later media was refreshed with puromycin at 2  $\mu$ g/mL; 24 h later, cells were infected with HCMV TB40/E at an MOI of 1. Lysates were collected at 4 DPI and (D) genome copy number and (E) viral titers were determined as described above. (A–E) Bars represent an average of three to six independent experiments and dots represent the data point for each replicate. Statistical significance was determined by two-tailed, paired *t* test with Bonferroni correction. Asterisks (\**P* < 0.01; \*\**P* < 0.001, \*\*\**P* < 0.0001) represent statistically significant differences determined in three or more independent experiments. (F) Fibroblasts uninfected or infected with HCMV at an MOI of 1. At 72 HPI, cells were fixed and processed for immunofluorescence. UL44 or Rev3L were indirectly detected using monoclonal antibodies to Rev3L or UL44 and secondary antibodies were conjugated to Alexa Fluor 546 (green) or 647 (red). Coverslips were imaged using a DeltaVision deconvolution microscope. A merged image with a high magnification. *Inset* of each channel plus DAPI staining to indicate nuclei is shown on the right of single-color panels.

infected cells, the spread of infection through the monolayer reflected differences in genome synthesis and virus replication for each set of knockdowns (*SI Appendix, Fig. S2C*). Depletion of pol( $\eta,\kappa,\iota$ ) resulted in increased spread of HCMV through the monolayer, whereas depletion of pol $\zeta$ /Rev1 restricted spread relative to the Luc knockdown control. From these data, we conclude that the effect of host cell polymerase depletion on HCMV genome synthesis and viral replication and is not due to defects in entry or initial events in infection prior to viral DNA synthesis.

**TLS Polymerases Differentially Impact the Replication of Other DNA Viruses.** Based on our findings in HCMV, we wondered if TLS polymerases are coopted by other dsDNA viruses which encode B-family polymerases. We examined HSV1, an  $\alpha$ -herpesvirus, and Vaccinia, a poxvirus that replicates its DNA in a specialized cytoplasmic compartment. Viral infections were performed on cells depleted of pol( $\eta,\kappa,\iota$ ), pol $\zeta$ /Rev1, or Luc. Based on the rapid lifecycles of both viruses, we performed low multiplicity infections (0.01 PFU per cell). We found that depletion of TLS polymerases affected HSV1, but to our surprise, in a diametric manner relative to HCMV. Depletion of pol $\zeta$ /Rev1 trended toward enhanced replication, however, due to wide variance was not significant (Fig. 4 *A* and *B*). Depletion of pol( $\eta,\kappa,\iota$ ) significantly diminished viral plaques, indicating these polymerases are required for optimal replication. Importantly, our knockdowns had no reproducible phenotypes on vaccinia replication (Fig. 4*C*), indicating that not all DNA viruses are equally dependent on TLS polymerases.

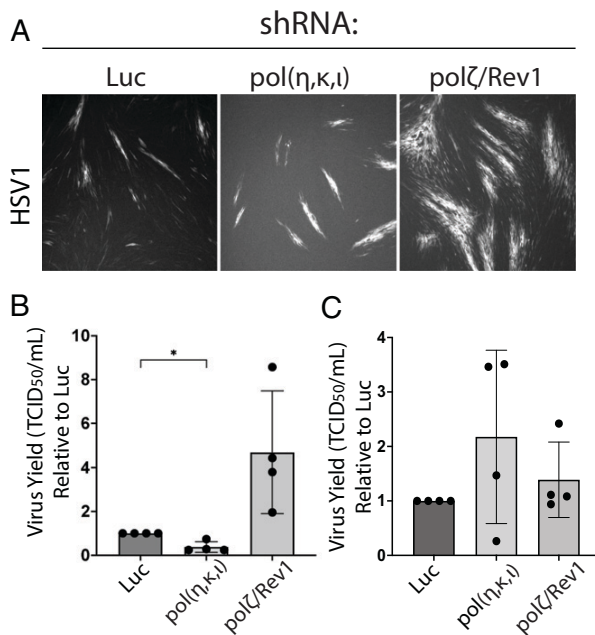


**Fig. 4.** Y-family polymerases differentially influence the replication of other DNA viruses. Growth-arrested fibroblasts were transduced with shRNA lentiviruses targeting Luc, insertion pol( $\eta,\kappa,\iota$ ) or postinsertion pol $\zeta$ /Rev1 at a cumulative MOI of 9. Forty-eight hours later media was refreshed with puromycin at 2  $\mu$ g/mL; 24 h later, cells were infected with HSV-1 (expressing GFP as a marker for infection) or vaccinia at an MOI of 0.01. (*A*) Images of the monolayer of cells infected with HSV1 at 33 HPI (200 $\times$ ). (*B* and *C*) Viral titers were measured at 33 HPI by TCID<sub>50</sub> for (*B*) HSV-1 and (*C*) vaccinia. Bars represent the average of four independent experiments and dots represent individual replicates. Statistical significance was determined by a two-tailed, paired *t* test with Bonferroni's correction. Asterisks ( $*P < 0.01$ ) represent statistically significant differences from the Luc control.

**TLS Polymerases Are Important for HCMV Genomic Stability.**

The observation that Y-family polymerases differentially affect viral replication and genome copy number suggests these TLS polymerases regulate viral DNA synthesis. Because TLS polymerases are known primarily to insert nucleotides across lesions or bypass lesions altogether during DNA replication, we hypothesized that depletion of TLS polymerases would compromise the fidelity of viral DNA synthesis (1, 33). To investigate the processes underlying the requirement of these TLS polymerases for viral DNA synthesis, we sequenced total genomic DNA from HCMV-infected cells depleted of Luc or an aggregate of pol( $\eta,\kappa,\iota$ ) or of pol $\zeta$ /Rev1. Sequence reads mapping to human reference genome were removed and the remaining reads were used to detect any alterations in HCMV genomes relative to the reference HCMV genome. Viral DNA, termed V1, was harvested from the viral stock used as the progenitor virus to infect shRNA-depleted cells and sequenced along with all other samples. This approach ensured that any preinfection genomic variants (e.g., HCMV polymorphisms or rearrangements) were identified and accounted for in subsequent genomic analysis.

We found that depletion of either pol( $\eta,\kappa,\iota$ ) or pol $\zeta$ /Rev1 resulted in a significant increase in genomic rearrangements, measured by the number and frequency of novel junctions detected in the viral genomes compared to the Luc knockdown control (Fig. 5 *A* and *B* and *SI Appendix, Fig. S3*). We also found that depletion of pol( $\eta,\kappa,\iota$ ) caused a significant decrease in the number of single nucleotide variants (SNVs: point mutations, deletions, or insertions) relative to the Luc knockdown control (Fig. 5*C* and *SI Appendix, Fig. S4*). Depletion of pol $\zeta$ /Rev1 resulted in a similar number SNVs relative to the Luc knockdown control. This observation is consistent with insertion polymerases having a higher error rate than B-family polymerases (29). The differences in number of novel junctions or SNVs among the shRNA conditions is not due to differences in sequence read depth, since read depth bias was accounted for by subsampling normalization (*SI Appendix, Materials and Methods* and Fig. S5). These data strikingly suggest that pol( $\eta,\kappa,\iota$ ) contribute to SNVs introduced during replication. Moreover, the increased level of de novo genomic rearrangements reflected in novel junctions strongly suggests that faithful HCMV genome replication and its stability requires host TLS polymerases.

Novel junctions relative to the V1 genome assemblies include inversions, duplications, and deletions, and we observed approximately the same fraction of junction types in each polymerase knockdown (*SI Appendix, Fig. S6 A and B*). Interestingly, we found that some junctions were present across all conditions, including the Luc shRNA control cells (Fig. 5 and *SI Appendix, Fig. S3*). Intercondition junctions (present in both Luc and all TLS knockdowns), likely indicate genomic sites that are inherently unstable. Of the six novel junction events detected in Luc control cells, three (50%) are junctions that were also observed in one or more other conditions (*SI Appendix, Figs. S3 and S6B*). In contrast, 75% and 76% of junctions were unique to either pol( $\eta,\kappa,\iota$ ) or pol $\zeta$ /Rev1 knockdowns, respectively (*SI Appendix, Fig. S6B*). Approximately 25% of novel junctions (absent in Luc control knockdown) were present in at least one replicate of both pol( $\eta,\kappa,\iota$ ) and pol $\zeta$ /Rev1 knockdowns. These inter-TLS junctions likely indicate sites in the viral genome that require the suite of TLS polymerases to maintain stability. Interestingly, 72% of novel pol( $\eta,\kappa,\iota$ ) junctions were unique to single replicates, while only 42% of these junctions observed in pol $\zeta$ /Rev1 knockdown were unique to single replicates. Thus, novel junctions in pol $\zeta$ /Rev1 knockdown cells are more numerous and tend to reoccur in more replicates. Therefore, depletion of pol $\zeta$ /Rev1 may result in a

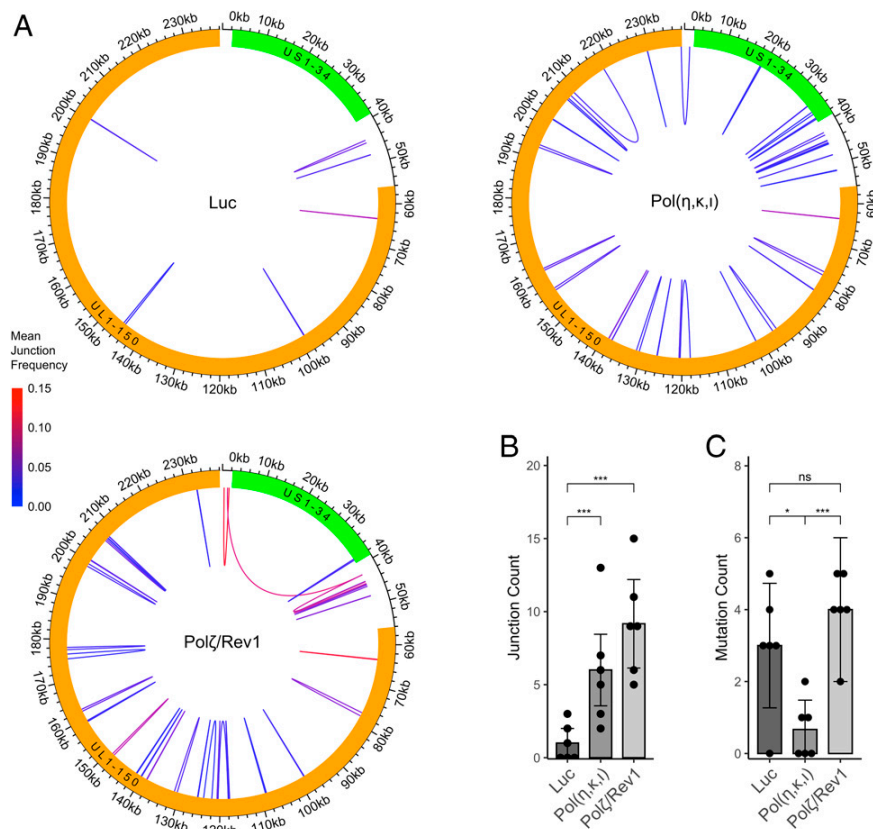


**Fig. 5.** Host TLS polymerases contribute to viral genome integrity. Growth-arrested fibroblasts were transduced with shRNA lentiviruses against Luc, insertion  $\text{pol}(\eta, \kappa, \iota)$ , or extension  $\text{pol}\zeta/\text{Rev}1$  at a cumulative MOI of 9. Forty-eight hours later, media was refreshed with puromycin at 2  $\mu\text{g}/\text{mL}$ ; 24 h later, cells were infected with HCMV at an MOI of 1 and total DNA was isolated at 4 DPI for sequencing. Sequences from each knockdown condition as well as from the V1 stock were aligned to the TB40/E-GFP reference genome sequence. (A) Mean novel junction frequency within each condition. HCMV genomic coordinates are plotted along the circular axis in graphs for Luc,  $\text{pol}(\eta, \kappa, \iota)$ , and  $\text{pol}\zeta/\text{Rev}1$  and the UL (orange) and US (green) regions of the genome are marked. The arcs connect novel junction points detected at the average frequency for the given condition indicated by the color scale. (B) Quantification of the number of novel junctions detected per sample ( $n = 6$ ) for each condition. (C) Quantification of the number of novel SNVs (point mutations, deletions, or insertions) detected per sample ( $n = 6$ ) for each condition. Statistical significance was determined by pairwise two-sided exact Poisson tests and adjusted using Bonferroni correction (ns,  $P > 0.05$ ; \* $P < 0.05$ ; \*\*\* $P < 0.001$ ).

greater instability burden at particular loci (*SI Appendix, Fig. S6B*). Importantly, in no cases did we observe specific novel junctions occurring in all six replicates, while more than half of all novel junctions (54%) occurred in only one replicate of one condition and 74% were condition-specific. These results suggest that novel junctions are indeed de novo HCMV rearrangements introduced during viral DNA synthesis, as opposed to preexisting low-copy number variants that undergo condition-specific selection.

We next examined the nature of the novel junctions and the sequences where they arise. The HCMV genome is ~57% GC-rich and contains repeated sequences of various lengths (34). Analysis of 20 bp on either side of each novel junction showed that  $\text{pol}\zeta/\text{Rev}1$ ,  $\text{pol}(\eta, \kappa, \iota)$ , or Luc-depleted cells joined sequences associated with repeated sequences (Fig. 6A) and contained 69%, 68%, and 68% GC content, respectively (Fig. 6B). Genomic regions in which novel junctions clustered had the highest GC content, some as high as 90% GC content (Fig. 6C and D and *SI Appendix, Fig. S6C*). However, when we only considered high-frequency novel junctions (junctions with  $\geq 25\%$  occurrence) within any one sample replicate, we found the average GC content of these genomic sites to be 75% ( $\pm 2.91\%$  SEM). Additionally, we noted that high-frequency novel junctions were enriched for repeated sequences (Fig. 6A). For example, when we examined 20-bp on either side of each novel junction, we found that 24% of all junctions

were associated with repeated sequences on at least one side of the novel junction, whereas 64% of high-frequency junctions were associated with repeated sequences on at least one side of the novel junction (Fig. 6A). Strikingly, in all conditions we found identical homologous sequences between sites generating novel junctions, and those sequences are always found precisely at only one side of the novel junction sequence (four examples shown in *SI Appendix, Fig. S6D–G*). Cumulatively, these findings suggest the HCMV genome contains common fragile sites, and that structural features such as regions of dense repeats or high GC content predispose viral chromatin to DNA repair or replicative processes that require host TLS polymerases.

The majority of junctions ( $\geq 70\%$ ) we observed resulted in mutations to viral genes. Particularly relevant are the viral genes that were mutated across both TLS knockdown conditions and not in Luc (inter-TLS), as these genes likely require the suite of TLS polymerases for their stability. Among these inter-TLS genes were UL50, UL80, and UL112, all of which are associated with viral replication or packaging (*SI Appendix, Table S1*) (34). We also observed inter-TLS junctions in UL27. Alternatively, some genes were unique to a single knockdown condition, indicating that only a particular set of TLS polys is required for its integrity, the most striking example being UL71, a tegument protein that was mutated in five of six  $\text{pol}\zeta/\text{Rev}1$  replicates. Taken together, these results indicate that HCMV fragile sites

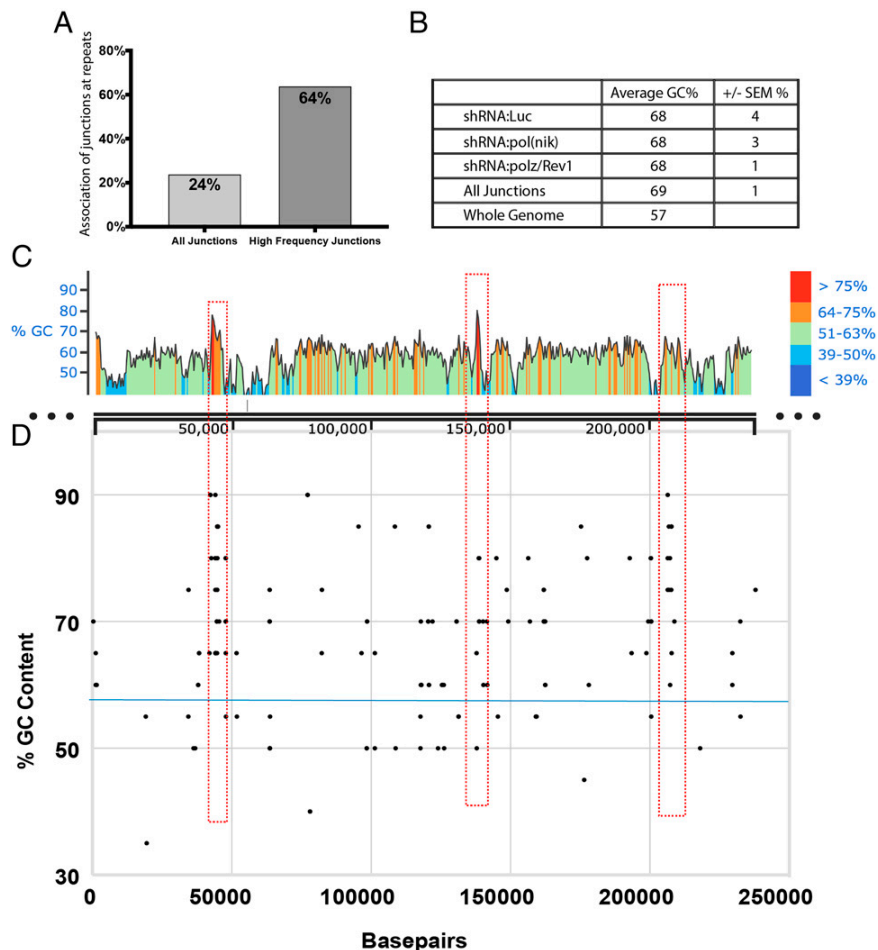


**Fig. 6.** HCMV genome rearrangement junction sites occur at GC-rich regions. (A) Proportion of novel junctions associated with repeat sequences, as defined by whether 20 bp on either side of the novel junction is found more than once in the reference genome with 100% identity. (B) Average percent GC content for whole HCMV reference genome and 20-nucleotides on both sides of novel junctions ( $\pm$ SEM, SEM). (C) Percent HCMV GC content and heat map calculated for 25-nucleotide sliding window (using Snappgene 6.0). (D) Percent GC content of each 20-nucleotide sequence flanking novel junctions plotted over their reference genome base pair coordinates. Blue horizontal line indicates 57% genome average GC content. Red dotted rectangles highlight regions of high GC content overlapping clusters of novel junctions.

are not limited to intergenic regions but instead represent structural motifs present in genes that are fundamental to the viral life cycle. Twenty-eight percent of all novel junctions joined intergenic regions, many within the internal and terminal repeat regions flanking the US and UL region of the genome. This observation suggests that TLS polymerase activity may be important to maintaining the structure of the genome in addition to preserving coding capacity.

## Discussion

All taxa encode DNA polymerases with specialized functions to allow organisms to respond to myriad challenges posed by genome replication and DNA repair to ensure genome integrity (6). Humans encode no less than 15 DNA polymerases, whose varied operation spans from processive synthesis to niche repair events (35). The orchestration of these polymerases is in part regulated by PCNA, whose posttranslational state controls Y-family polymerase recruitment (36, 37). While the regulation and specificity of Ub-PCNA and TLS polymerases for synthesis and repair in eukaryotes is not yet fully elucidated, much less is known regarding the importance of these systems for DNA virus replication, particularly where the virus encodes its own polymerase and

processivity factor. It has been presumed that viral polymerases are sufficient for the synthesis of viral genomes. However, it is not clear how a single viral polymerase can achieve what requires 15 polymerases in a cell. This work demonstrates that the HCMV polymerase, UL54, is not sufficient for viral DNA synthesis and that host TLS polymerases are necessary for viral genome stability.

We observed redistribution of TLS polymerases and modification of their regulator, Ub-PCNA, in HCMV infection and accordingly investigated the importance of TLS polymerases for the HCMV life cycle. We found that depletion of pol $\eta$ , pol $\kappa$ , and pol $\iota$  in aggregate enhanced HCMV replication. Conversely, depletion of pol $\zeta$  (Rev3L and Rev7) and Rev1, restricted viral replication, indicating an exciting diversity of host polymerase function in HCMV DNA replication. Short-read sequencing revealed that both cohorts of TLS polymerases are required to maintain HCMV genomic integrity, and that pol $\eta$ , pol $\kappa$ , and pol $\iota$  are responsible for a significant proportion of SNVs in the HCMV genome that occur during synthesis. TLS-mediated generation of SNVs on the viral genome may contribute to viral diversity and evolutionary fitness, reflecting the role of TLS polymerases in generating immunoglobulin diversity by somatic hypermutation in vertebrates (38). Intriguingly, in HSV-1 infection, we found the same polymerases exerted an opposite effect,

indicating that host polymerases and associated machinery may be important for numerous DNA viruses, but their contributions could differ radically. These observations highlight the importance of TLS polymerases in the viral life cycle, although the precise role for each TLS polymerase remains to be determined.

TLS studies conducted from yeast to human cancers indicate a stepwise process for lesion bypass, one wherein Ub-PCNA recruits Y-family polymerases to insert opposite the lesion and extension is mediated by pol $\zeta$ /Rev1 (39, 40). In instances where any of these subunits are targeted, the phenotypic outcome ranges between increased mutational burden to cell death likely resulting from double-stranded breaks and failure to resolve lesions (39). Therefore, we had anticipated that if any TLS polymerase affected HCMV replication, other TLS polymerases would exert a similar phenotype. Curiously, this is not what we found. Rather, our evidence suggests that pol $\eta$ , pol $\kappa$ , and pol $\iota$ , normally function to restrict HCMV viral DNA synthesis and replication, while Rev1 and pol $\zeta$  are important for optimal viral DNA synthesis and replication. Importantly, this diametric outcome does not appear to be arbitrary but instead divided by function: insertion polymerases versus extension polymerases and associated partners.

One explanation for the suppression of viral replication observed with pol( $\eta,\kappa,\iota$ ) depletion is that TLS polymerases perform their canonical function with the consequence of slowed replication rates. In support, *Escherichia coli* Y-family polymerases, polIII and polIV, can retard the rate of the helicase unwinding to as little as 1 bp/s, thereby decreasing replication kinetics, possibly allowing for excision repair systems to correct errors (41). In line with this it is interesting to note that depletion of pol( $\eta,\kappa,\iota$ ) decreased SNV numbers (Fig. 5C). This finding suggests that pol $\eta$ , pol $\kappa$ , and pol $\iota$  actively incorporate nucleotides in the viral genome and do so with an increased error rate. Therefore, it is conceivable that pol $\eta$ , pol $\kappa$ , and pol $\iota$  hamper replicon speed via increased necessity for polymerase editing functions and mismatch repair while decreasing helicase kinetics. In contrast to its well-described role in TLS, pol $\eta$  also contributes to lagging strand synthesis on undamaged DNA in competition with pol $\delta$  and pol $\alpha$  in *Saccharomyces cerevisiae*, which confers a mutational cost and could slow bulk synthesis (42).

Our short-read sequencing revealed significant increases in both the number and frequencies of HCMV genome rearrangement in TLS polymerase knockdowns. Importantly, most of these mutations were associated with GC-rich regions and sites of repeated sequences (Fig. 6 and *SI Appendix*, Fig. S6). We draw two conclusions from these findings. First, the viral genome is not uniformly stable, thus revealing possible common fragile sites with inherently unstable sequences. Second, TLS polymerases are required to maintain stability at particular genetic loci while also facilitating or restricting DNA replication. Indeed, GC- and repeat-rich DNA is inherently unstable; both genomic features positively correlate with DNA lesions, such as alkylation, and both are subject to increased deletions, duplication, and recombination events arising from associated repair processes (43–45). We observed these mutation types in TLS polymerase-depleted cells and their abundance correlated with both GC content and repeats, indicating that TLS polymerases are necessary to mitigate genomic instability associated with these inherently unstable regions.

In support of this idea, we observed that about half of all genome rearrangements occurred in more than one biological replicate regardless of condition (*SI Appendix*, Figs. S3 and S6B). Additionally, the increase in junction count in the pol $\zeta$ /Rev1-depleted cells relative to Luc control and pol( $\eta,\kappa,\iota$ )-depleted cells results not from an increase in unique junctions, but from a

recurrence of the same junctions in multiple replicates (*SI Appendix*, Figs. S3 and S6B). It is important to note that junction frequency alone is an elusive metric for the significance of TLS polymerases, as high-frequency junctions may reflect a single mutational event that occurred early in infection and was amplified over subsequent rounds of replication. Therefore, the recurrence of the same junctions over multiple replicates, and less so their individual frequencies, strongly suggests that recurring HCMV genomic rearrangements represent independent de novo DNA recombination junctions that arise from fragile sites normally suppressed by TLS polymerase activities.

Importantly, many of the fragile sites we observed were not confined to intergenic regions, but rather genes that are important for the viral life cycle. While our study did not assess the outcomes of such mutations on gene expression, packaging, or subsequent infections, it is likely that the mutations we observed would negatively influence these processes and may contribute to the replicative phenotypes we observed (Figs. 2–4). Among the fragile sites observed, UL27 is a gene that, when mutated, can confer modest resistance to the antiviral maribavir (46, 47). Because TLS pols have a higher intrinsic error rate, genes such as UL27 could be subject to increased SNV burdens and therefore may act as sites of rapid evolutionary selection (1). Numerous SNVs in UL27 have been shown to render progeny virus resistant to maribavir (46).

While we are unable to define the exact damage and repair processes that lead to these junctional outcomes, the types of mutations we observed are consistent with defects in homology-directed repair (HDR). Importantly, TLS activity regulates HDR, and there is increasing evidence that HDR requires TLS polymerases. In TLS-deficient systems, DNA lesions cause replicon skipping, leading to single-stranded DNA (ssDNA) gaps (48). In the absence of TLS polymerases, ssDNA regions are resolved using RAD51- and RAD52-dependent HDR; however, this repair process is associated with increased mutagenic recombination, indicating TLS polymerases are also required for accurate homologous recombination (HR) (49). Our observations agree with these findings, as we observe increased junctional mutations consistent with hobbled HDR.

Interestingly, while insertion polymerases, such as pol $\eta$ , and postinsertion polymerases, such as pol $\zeta$ , have been reported as contributing to HDR, there is evidence that pol $\zeta$ , in coordination with Rev1, plays a more significant role in HDR. In *S. cerevisiae*, pol $\zeta$  contributes to HDR and is responsible for ~95% of mutations observed at repair sites (28). More recently, *in vitro* studies conducted on synthetic D-loops indicated that pol $\zeta$  can partially extend through D-loops (29). Finally, gap repair assays in *Drosophila melanogaster* indicate that pol $\zeta$ , and to a lesser extent pol $\eta$ , contribute to HR, underscoring their importance when ssDNA gaps are present, such as following lesion skipping (50). Taken together, these data indicate an increased dependence on pol $\zeta$  for accurate HDR and may explain why depletion of pol $\zeta$  and its effectors is deleterious for viral replication.

The marriage of our observations and the literature led us to propose that the GC- and repeat-rich environment of herpes viral genomes are subject to increased lesions and damage necessitating bypass (43, 44). We propose that HCMV employs TLS polymerases to perform their canonical function in lesion bypass, as evidenced by the decrease in SNV frequency upon depletion of pol( $\eta,\kappa,\iota$ ) (Fig. 5B). The cost of increased TLS activity, however, is decreased replicon speed, thereby suppressing viral replication rates (41, 51). Our data further indicate that TLS polymerases are not merely limited to canonical bypass, but that pol $\zeta$ /Rev1 plays an integral role in accurately guiding HDR when necessary, and



therefore the loss of Rev3L, Rev1, or Rev7 diminishes viral replication (Fig. 3).

It is worthwhile to speculate what, if any, advantages come of a DNA architecture prone to increased lesions, as with herpesviruses. One intriguing possibility is that of promoting increased break-induced replication (BIR, also known as recombination-dependent replication), a particular brand of HR necessary for  $\lambda$  bacteriophage replication (36, 37, 52). Indeed, increasing evidence supports that HSV1 also employs break-induced recombination for replication, underscoring the possibility that HCMV employs the same strategy (39, 40). Intriguingly, our results indicate that TLS pols suppress BIR in infection, as depletion of TLS pols yielded junctions with repair signatures conforming to BIR (*SI Appendix, Fig. S6*). We observed short stretches of sequence homology shared between recombining sites, and this homology was always found only on one side of novel junctions (*SI Appendix, Fig. S6 D–G*). BIR mechanisms are known to use homology on one side of a break to initiate strand invasion and synthesis (53). In the presence of TLS polymerases, dNTPs are incorporated opposite a lesion or they are bypassed altogether (9, 54), whereas in the absence of TLS activities, DNA lesions can trigger HDR (49). It is possible that in the absence of TLS activities, HCMV DNA replication cannot proceed through GC-rich DNA repeats or structures. For example, in yeast pol $\zeta$  is required for replication through GC-rich interstitial telomeric sequences (55), and such sequences are associated with human genome fragile sites (56). In the absence of TLS activities, failing to bypass such lesions then allows HDR to avail itself of the abundant viral genome copies or repeat sequences dispersed throughout the HCMV genome. Significant work remains, however, to understand precisely what type of lesions persist in the absence of TLS polymerases and exactly what repair and replication mechanisms prevail in their absence.

Like CMV, HSV has a similar set of challenges for DNA replication; indeed, HSV has greater GC content (57, 58), and studies of viral replication indicate GC-rich regions, such as the thymidine kinase gene, are mutational hotspots, possibly due to polymerase slippage (59). Curiously, while we found that TLS pols affect HSV-1 replication, they do so diametrically compared to CMV, where pol( $\eta, \kappa, \iota$ ) was necessary for optimal replication, and pol $\zeta$ /Rev1 tended toward restriction (Fig. 4). Importantly, our findings are consistent with previous work examining the contributions of pol $\eta$  in HSV replication. However, while these studies also concluded that pol $\eta$  is critical for HSV replication, they did not explore the effects of other TLS pols (60). It is unclear why depletion of TLS pols provides such divergent replication phenotypes, and it is possible that in both HSV and CMV TLS pols are regulating a class of activity distinct from DNA replication, such as gene expression or signaling.

Accurate DNA replication is an imperative shared by all organisms. So variable and complex is this task, that an ever-expanding cast of molecules is required to maintain genomic integrity. Curiously, in stark contrast to bacteria, fungi, and animals, dsDNA viruses encode at most a single polymerase, one that by its very fidelity and speed is incapable of performing lesion bypass (1, 61, 62). The importance of host TLS polymerases for viral replication is increasingly appreciated; TLS polymerases contribute to HSV1, Epstein-Barr virus, and even ssDNA virus of the Gemini family replication, although the consequences for loss of this activity is not well-defined (63–65). Our work suggests that complex herpesviruses coopt multiple host polymerases for specialized repair and synthesis events that impact viral genome integrity. It will be of interest to further elucidate the biological relevance of HCMV genomic sites that appear to be inherently unstable and how TLS

polymerases function to mitigate their instability. We anticipate our work will expand the narrative for how dsDNA viruses replicate. Furthermore, it raises the possibility that viral infection recruits TLS functions away from host genomes and may have consequences for host genomic integrity. Finally, we hope our findings may provide useful insight into the ever-expanding roles of TLS polymerases in DNA replication and repair.

## Materials and Methods

**Cells and Virus.** Primary lung MRC-5 fibroblasts (ATCC CCL-171) were maintained as previously described (66, 67). Cells were infected with a low-passage strain of HCMV, TB40/E, a gift from Christian Sinzger (University Hospital Ulm, Ulm, Germany) (68), which expresses the green fluorescent protein as a marker for infection (69). For HSV-1 and Vaccinia infection, the HSV-1 strain F (a gift from Janko Nikolich-Zugich, University of Arizona, Tucson, AZ) was constructed by David Johnson's laboratory (University Hospital Ulm, Ulm, Germany) and expresses glycoprotein E fused with GFP (70) and Vaccinia Western Reserve strain (a gift from Grant McFadden, Arizona State University, Tucson, AZ) was used to infect MRC-5 cells. In brief, infectious inoculum was added to cultured medium and agitated once every 15 min for 1 to 2 h. Next, inoculum was removed, cells were washed 3 $\times$  in Dulbecco's phosphate-buffered saline (PBS) then provided fresh DMEM containing 10% FBS.

**Immunoblotting.** Immunoblotting was performed as previously described (71). Briefly, 25 to 50  $\mu$ g of protein lysate was separated on 12% bis-Tris gels by electrophoresis and transferred to 0.45- $\mu$ m-pore size polyvinylidene difluoride (Immobilon-FL; Millipore) membranes. Proteins were detected using epitope- or protein-specific antibodies and fluorescently conjugated secondary antibodies using an Odyssey infrared imaging system (Li-Cor). All antibodies used are described in *SI Appendix, Table S3*. Protein levels were quantitated using LiCor Image Studio Lite software in the linear range.

**Next-Generation Sequencing and Computational Analysis.** Six replicate samples from each knockdown plus infection were sequenced on a NextSeq 2000 Illumina short-read sequencer to yield paired-end short reads. Reads remaining after removal of reads mapping to the human genome were aligned to reference HCMV genome with breseq v0.36.0 (72) using the polymorphism-prediction mode. The novel junctions and SNVs were obtained by removing any of those found in the V1 sample (without subsampling of sequencing reads) from the total junctions and SNVs detected in each experimental sample (after subsampling). Subsequent data analysis was completed in R v4.0.2. By scanning the junction DNA sequences using the Biostrings (73) library, percent GC content of the 20-bp sequences surrounding junctions was determined and searched for identical matches within the reference HCMV genome to determine copy number for each 20-bp junction proximal sequence.

**Data Availability.** Alignments used for Fig. 5 and a TB40E reference genome are available at the University of Arizona Research Data Repository: doi:10.25422/azu.data.19127993 (74). Raw sequence reads have been deposited in the Sequence Read Archive, <https://www.ncbi.nlm.nih.gov/sra> (BioProject ID: PRJNA804561) (75). Please see *SI Appendix* for a detailed description of the materials and methods.

**ACKNOWLEDGMENTS.** We thank Drs. Sandy Weller (University of Connecticut), Jill Dembowski (Duquesne University), Kareem Mohni (Mayo Clinic, Rochester), Moriah Szpara (Pennsylvania State University), James Alwine (University of Pennsylvania) and Lynn Enquist (Princeton University) for informative and critical discussion; Dr. Janko Nikolich-Zugich (University of Arizona) and Dr. Grant McFadden (Arizona State University) for the gift of viruses; and Dr. Ross Buchan (University of Arizona) for use of and assistance with the DeltaVision deconvolution microscope. This work was supported by Public Health Service Grants A1079059 and A127335 (to F.G.), and a Diversity supplement on A1079059 (to F.G./P.L.) from the National Institute of Allergy and Infectious Disease; Geisel School of Medicine research funds (G.B.); and Burroughs Wellcome Fund-Big Data in the Life Sciences Training Program at Dartmouth (M.S.). This work was also supported, in part, by the Cytometry Shared Resource, University of Arizona Cancer Center (P30CA023074).

1. M. F. Goodman, R. Woodgate, Translesion DNA polymerases. *Cold Spring Harb. Perspect. Biol.* **5**, a010363 (2013).
2. A. Bbenek, I. Ziuzia-Graczyk, Fidelity of DNA replication—a matter of proofreading. *Curr. Genet.* **64**, 985–996 (2018).
3. S. Xia, W. H. Konigsberg, RB69 DNA polymerase structure, kinetics, and fidelity. *Biochemistry* **53**, 2752–2767 (2014).
4. H. Ling, F. Boudsoq, R. Woodgate, W. Yang, Crystal structure of a Y-family DNA polymerase in action: A mechanism for error-prone and lesion-bypass replication. *Cell* **107**, 91–102 (2001).
5. S. Sertic *et al.*, Coordinated activity of Y family TLS polymerases and EXO1 protects non-S phase cells from UV-induced cytotoxic lesions. *Mol. Cell* **70**, 34–47.e4 (2018).
6. S. Sharma, C. E. Canman, REV1 and DNA polymerase zeta in DNA interstrand crosslink repair. *Environ. Mol. Mutagen.* **53**, 725–740 (2012).
7. W. Yang, R. Woodgate, What a difference a decade makes: Insights into translesion DNA synthesis. *Proc. Natl. Acad. Sci. U.S.A.* **104**, 15591–15598 (2007).
8. J. E. Sale, A. R. Lehmann, R. Woodgate, Y-family DNA polymerases and their role in tolerance of cellular DNA damage. *Nat. Rev. Mol. Cell Biol.* **13**, 141–152 (2012).
9. A. V. Makarova, P. M. Burgers, Eukaryotic DNA polymerase  $\zeta$ . *DNA Repair (Amst.)* **29**, 47–55 (2015).
10. W. Yang, Y. Gao, Translesion and repair DNA polymerases: Diverse structure and mechanism. *Annu. Rev. Biochem.* **87**, 239–261 (2018).
11. M. W. Czarnecki, P. Traktman, The vaccinia virus DNA polymerase and its processivity factor. *Virus Res.* **234**, 193–206 (2017).
12. K. Zarrouk, J. Piret, G. Boivin, Herpesvirus DNA polymerases: Structures, functions and inhibitors. *Virus Res.* **234**, 177–192 (2017).
13. J. Trimpert *et al.*, A proofreading-impaired herpesvirus generates populations with quasispecies-like structure. *Nat. Microbiol.* **4**, 2175–2183 (2019).
14. D. M. Coen, J. L. Lawler, J. Abraham, Herpesvirus DNA polymerase: Structures, functions, and mechanisms. *Enzymes* **50**, 133–178 (2021).
15. S. Ravichandran *et al.*, Genome-wide analysis of regulatory G-quadruplexes affecting gene expression in human cytomegalovirus. *PLoS Pathog.* **14**, e1007334 (2018).
16. M. Schmid, T. Speiseder, T. Dobner, R. A. Gonzalez, DNA virus replication compartments. *J. Virol.* **88**, 1404–1420 (2014).
17. B. L. Strang, Viral and cellular subnuclear structures in human cytomegalovirus-infected cells. *J. Gen. Virol.* **96**, 239–252 (2015).
18. E. Caragliano *et al.*, Human cytomegalovirus forms phase-separated compartments at viral genomes to facilitate viral replication. *Cell Rep.* **38**, 110469 (2022).
19. E. Xiaofei *et al.*, A novel DDB2-ATM feedback loop regulates human cytomegalovirus replication. *J. Virol.* **88**, 2279–2290 (2014).
20. J. M. O'Dowd, A. G. Zavala, C. J. Brown, T. Mori, E. A. Fortunato, HCMV-infected cells maintain efficient nucleotide excision repair of the viral genome while abrogating repair of the host genome. *PLoS Pathog.* **8**, e1003038 (2012).
21. E. Xiaofei, T. F. Kowalik, The DNA damage response induced by infection with human cytomegalovirus and other viruses. *Viruses* **6**, 2155–2185 (2014).
22. J. Cudini *et al.*, Human cytomegalovirus haplotype reconstruction reveals high diversity due to superinfection and evidence of within-host recombination. *Proc. Natl. Acad. Sci. U.S.A.* **116**, 5693–5698 (2019).
23. F. Lassalle *et al.*, Islands of linkage in an ocean of pervasive recombination reveals two-speed evolution of human cytomegalovirus genomes. *Virus Evol.* **2**, vew017 (2016).
24. S. Sijmons *et al.*, High-throughput analysis of human cytomegalovirus genome diversity highlights the widespread occurrence of gene-disrupting mutations and pervasive recombination. *J. Virol.* **89**, 7673–7695 (2015).
25. L. S. Waters *et al.*, Eukaryotic translesion polymerases and their roles and regulation in DNA damage tolerance. *Microbiol. Mol. Biol. Rev.* **73**, 134–154 (2009).
26. B. L. Strang *et al.*, Human cytomegalovirus UL44 concentrates at the periphery of replication compartments, the site of viral DNA synthesis. *J. Virol.* **86**, 2089–2095 (2012).
27. S. Sharma *et al.*, REV1 and polymerase  $\zeta$  facilitate homologous recombination repair. *Nucleic Acids Res.* **40**, 682–691 (2012).
28. S. L. Holbeck, J. N. Strathern, A role for REV3 in mutagenesis during double-strand break repair in *Saccharomyces cerevisiae*. *Genetics* **147**, 1017–1024 (1997).
29. J. Li, D. L. Holzschu, T. Sugiyama, PCNA is efficiently loaded on the DNA recombination intermediate to modulate polymerase  $\delta$ ,  $\eta$ , and  $\zeta$  activities. *Proc. Natl. Acad. Sci. U.S.A.* **110**, 7672–7677 (2013).
30. R. P. Anand *et al.*, Chromosome rearrangements via template switching between diverged repeated sequences. *Genes Dev.* **28**, 2394–2406 (2014).
31. R. E. Johnson, M. T. Washington, L. Haracska, S. Prakash, L. Prakash, Eukaryotic polymerases  $\iota$  and  $\zeta$  act sequentially to bypass DNA lesions. *Nature* **406**, 1015–1019 (2000).
32. D. K. Rajpal, X. Wu, Z. Wang, Alteration of ultraviolet-induced mutagenesis in yeast through molecular modulation of the REV3 and REV7 gene expression. *Mutat. Res.* **461**, 133–143 (2000).
33. O. Ziv, N. Geacintov, S. Nakajima, A. Yasui, Z. Livneh, DNA polymerase zeta cooperates with polymerases kappa and  $\iota$  in translesion DNA synthesis across pyrimidine photodimers in cells from XPV patients. *Proc. Natl. Acad. Sci. U.S.A.* **106**, 11552–11557 (2009).
34. F. Goodrum, W. Britt, E. S. Mocarski, "Cytomegalovirus" in *Fields Virology: DNA Viruses*, P. M. Howley, D. M. Knipe, J. L. Cohen, B. A. Damania, Eds. (Wolters Kluwer, 2022), vol. 2, chap. 12.
35. K. Chan, M. A. Resnick, D. A. Gordenin, The choice of nucleotide inserted opposite abasic sites formed within chromosomal DNA reveals the polymerase activities participating in translesion DNA synthesis. *DNA Repair (Amst.)* **12**, 878–889 (2013).
36. L. W. Enquist, A. Skalka, Replication of bacteriophage lambda DNA dependent on the function of host and viral genes. I. Interaction of red, gam and rec. *J. Mol. Biol.* **75**, 185–212 (1973).
37. D. E. Wilkinson, S. K. Weller, The role of DNA recombination in herpes simplex virus DNA replication. *IUBMB Life* **55**, 451–458 (2003).
38. J. U. Peled *et al.*, The biochemistry of somatic hypermutation. *Annu. Rev. Immunol.* **26**, 481–511 (2008).
39. S. Weerasooriya, K. A. DiScipio, A. S. Darwish, P. Bai, S. K. Weller, Herpes simplex virus 1 ICP8 mutant lacking annealing activity is deficient for viral DNA replication. *Proc. Natl. Acad. Sci. U.S.A.* **116**, 1033–1042 (2019).
40. L. M. Grady *et al.*, The exonuclease activity of herpes simplex virus 1 UL12 is required for production of viral DNA that can be packaged to produce infectious virus. *J. Virol.* **91**, e01380-17 (2017).
41. C. Indiani, L. D. Langston, O. Yurieva, M. F. Goodman, M. O'Donnell, Translesion DNA polymerases remodel the replisome and alter the speed of the replicative helicase. *Proc. Natl. Acad. Sci. U.S.A.* **106**, 6031–6038 (2009).
42. K. Kreisel *et al.*, DNA polymerase  $\eta$  contributes to genome-wide lagging strand synthesis. *Nucleic Acids Res.* **47**, 2425–2435 (2019).
43. D. A. Kiktev, Z. Sheng, K. S. Lobachev, T. D. Petes, GC content elevates mutation and recombination rates in the yeast *Saccharomyces cerevisiae*. *Proc. Natl. Acad. Sci. U.S.A.* **115**, E7109–E7118 (2018).
44. W. B. Mattes, J. A. Hartley, K. W. Kohn, D. W. Matheson, GC-rich regions in genomes as targets for DNA alkylation. *Carcinogenesis* **9**, 2065–2072 (1988).
45. A. R. Poetsch, S. J. Boulton, N. M. Luscombe, Genomic landscape of oxidative DNA damage and repair reveals regioselective protection from mutagenesis. *Genome Biol.* **19**, 215 (2018).
46. S. Chou, G. I. Marousek, A. E. Senter, M. G. Davis, K. K. Biron, Mutations in the human cytomegalovirus UL27 gene that confer resistance to maribavir. *J. Virol.* **78**, 7124–7130 (2004).
47. J. M. Reitsma *et al.*, Antiviral inhibition targeting the HCMV kinase pUL97 requires pUL27-dependent degradation of Tip60 acetyltransferase and cell-cycle arrest. *Cell Host Microbe* **9**, 103–114 (2011).
48. S. Chang *et al.*, A gatekeeping function of the replicative polymerase controls pathway choice in the resolution of lesion-stalled replisomes. *Proc. Natl. Acad. Sci. U.S.A.* **116**, 25591–25601 (2019).
49. W. Ma, J. W. Westmoreland, M. A. Resnick, Homologous recombination rescues ssDNA gaps generated by nucleotide excision repair and reduced translesion DNA synthesis in yeast G2 cells. *Proc. Natl. Acad. Sci. U.S.A.* **110**, E2895–E2904 (2013).
50. D. P. Kane, M. Shusterman, Y. Rong, M. McVey, Competition between replicative and translesion polymerases during homologous recombination repair in *Drosophila*. *PLoS Genet.* **8**, e1002659 (2012).
51. J. E. Kath *et al.*, Polymerase exchange on single DNA molecules reveals processivity clamp control of translesion synthesis. *Proc. Natl. Acad. Sci. U.S.A.* **111**, 7647–7652 (2014).
52. G. Bosco, J. E. Haber, Chromosome break-induced DNA replication leads to nonreciprocal translocations and telomere capture. *Genetics* **150**, 1037–1047 (1998).
53. J. Kramara, B. Osia, A. Malkova, Break-induced replication: The where, the why, and the how. *Trends Genet.* **34**, 518–531 (2018).
54. C. J. Sakofsky *et al.*, Translesion polymerases drive microhomology-mediated break-induced replication leading to complex chromosomal rearrangements. *Mol. Cell* **60**, 860–872 (2015).
55. A. Moore *et al.*, Genetic control of genomic alterations induced in yeast by interstitial telomeric sequences. *Genetics* **209**, 425–438 (2018).
56. A. Y. Aksenova, S. M. Mirkin, At the beginning of the end and in the middle of the beginning: Structure and maintenance of telomeric DNA repeats and interstitial telomeric sequences. *Genes (Basel)* **10**, 118 (2019).
57. D. J. McGeoch *et al.*, The complete DNA sequence of the long unique region in the genome of herpes simplex virus type 1. *J. Gen. Virol.* **69**, 1531–1574 (1988).
58. D. J. McGeoch, A. Dolan, S. Donald, D. H. Brauer, Complete DNA sequence of the short repeat region in the genome of herpes simplex virus type 1. *Nucleic Acids Res.* **14**, 1727–1745 (1986).
59. D. Chibo, J. Druce, J. Sasadeusz, C. Birch, Molecular analysis of clinical isolates of acyclovir resistant herpes simplex virus. *Antiviral Res.* **61**, 83–91 (2004).
60. I. Muylaert, P. Elias, Contributions of nucleotide excision repair, DNA polymerase  $\eta$ , and homologous recombination to replication of UV-irradiated herpes simplex virus type 1. *J. Biol. Chem.* **285**, 13761–13768 (2010).
61. L. A. Loeb, R. J. Monnat Jr., DNA polymerases and human disease. *Nat. Rev. Genet.* **9**, 594–604 (2008).
62. V. Khare, K. A. Eckert, The proofreading 3'→5' exonuclease activity of DNA polymerases: A kinetic barrier to translesion DNA synthesis. *Mutat. Res.* **510**, 45–54 (2002).
63. K. S. Richter, M. Götz, S. Winter, H. Jeske, The contribution of translesion synthesis polymerases on geminiviral replication. *Virology* **488**, 137–148 (2016).
64. O. F. Dyson, J. S. Pagano, C. B. Whitehurst, The translesion polymerase pol  $\eta$  is required for efficient Epstein-Barr virus infectivity and is regulated by the viral deubiquitinating enzyme BPLF1. *J. Virol.* **91**, e00600-17 (2017).
65. X. Dong, J. Guan, C. Zheng, X. Zheng, The herpes simplex virus 1 UL36USP deubiquitinase suppresses DNA repair in host cells via deubiquitination of proliferating cell nuclear antigen. *J. Biol. Chem.* **292**, 8472–8483 (2017).
66. K. Caviness, L. Cicchini, M. Rak, M. Umashankar, F. Goodrum, Complex expression of the UL136 gene of human cytomegalovirus results in multiple protein isoforms with unique roles in replication. *J. Virol.* **88**, 14412–14425 (2014).
67. M. Umashankar *et al.*, Antagonistic determinants controlling replicative and latent states of human cytomegalovirus infection. *J. Virol.* **88**, 5987–6002 (2014).
68. C. Sinzger *et al.*, Cloning and sequencing of a highly productive, endotheliotropic virus strain derived from human cytomegalovirus TB40/E. *J. Gen. Virol.* **89**, 359–368 (2008).
69. M. Umashankar *et al.*, A novel human cytomegalovirus locus modulates cell type-specific outcomes of infection. *PLoS Pathog.* **7**, e1002444 (2011).
70. A. Farnsworth, K. Goldsmith, D. C. Johnson, Herpes simplex virus glycoproteins gD and gE/gI serve essential but redundant functions during acquisition of the virion envelope in the cytoplasm. *J. Virol.* **77**, 8481–8494 (2003).
71. A. Petrucelli, M. Rak, L. Grainger, F. Goodrum, Characterization of a novel Golgi apparatus-localized latency determinant encoded by human cytomegalovirus. *J. Virol.* **83**, 5615–5629 (2009).
72. D. E. Deatherage, C. C. Travers, L. N. Wolf, J. E. Barrick, Detecting rare structural variation in evolving microbial populations from new sequence junctions using breseq. *Front. Genet.* **5**, 468 (2015).
73. H. Pages, P. Aboyoun, R. Gentleman, S. DebRoy, Biostrings: Efficient manipulation of biological strings (R package version 2.62.0, 2021) <https://bioconductor.org/packages/release/bioc/html/Biostrings.html>. Accessed 13 July 2021.
74. S. Zeltzer, P. Longmire, M. Svoboda, G. Bosco, F. Goodrum, Alignment data for "Host translesion polymerases are required for viral genome integrity." University of Arizona Research Data Repository. <http://doi.org/10.25422/azu.data.19127993>. Deposited 2 June 2022.
75. S. Zeltzer, P. Longmire, M. Svoboda, G. Bosco, F. Goodrum, Raw sequence reads for "Host translesion polymerases are required for viral genome integrity." NCBI Sequence Read Archive. <http://www.ncbi.nlm.nih.gov/bioproject/804561>. Deposited 27 July 2022.